Bioorganic Chemistry 111 (2021) 104841

Contents lists available at ScienceDirect

Bioorganic Chemistry

journal homepage: www.elsevier.com/locate/bioorg

Design, synthesis and mechanistic study of new 1,2,4-triazole derivatives as antimicrobial agents

Noha H. Amin [a,*], Mohamed T. El-Saadi [a,b], Ahmed A. Ibrahim [c], Hamdy M. Abdel-Rahman [c,d]

[a] Department of Medicinal Chemistry, Faculty of Pharmacy, Beni-Suef University, Beni-Suef 62514, Egypt
[b] Department of Medicinal Chemistry, Faculty of Pharmacy, Sinai University-Kantra Branch, Egypt
[c] Department of Pharmaceutical Chemistry, Faculty of Pharmacy, Nahda University, Beni-Suef, Egypt
[d] Department of Medicinal Chemistry, Faculty of Pharmacy, Assiut University, 71526 Assiut, Egypt

ARTICLE INFO

Keywords:
1,2,4-Triazoles
1,2,4-Triazolo[1,5-*a*]pyrimidines
Lansterol 14α-demethylase
Antimicrobial
Antifungal

ABSTRACT

Novel 5-amino-1,2,4-triazole derivatives and their cyclized 1,2,4-triazolo[1,5-*a*]pyrimidine analogues were designed, synthesized and evaluated for their antimicrobial activities. They were tested against five bacterial strains (Methicillin Resistant *S. aureus* (MRSA), *E. coli, K. pneumoniae, A. baumannii* and *P. aeruginosa)* using ciprofloxacin as a positive control and against two fungal strains (*C. albicans* and *C. neoformans*) using fluconazole and amphotericin B as positive controls. Compounds **9, 13a** and **13b** showed high to moderate antifungal activities against *candida albicans* (MIC values = 4–32 μg/ml), with considerable safety profiles; where no cytotoxicity against human embryonic kidney or red blood cells were detected at concentrations up to 32 μg/mL. Furthermore, compound **9** showed significant inhibitory activity against lansterol 14α-demethylase (IC_{50} = 0.27 μM), compared to the reference drug fluconazole (IC_{50} = 0.25 μM). Molecular docking of compound **9** into the active site of the cytochrome P450 enzyme revealed comparable binding modes and docking scores to those of fluconazole. Finally, *in silico* ADME studies prediction and drug-like properties of these compounds revealed favorable oral bioavailability results.

1. Introduction

Microbial infections have ever since become a burden on all health care systems and one of the major life threatening problems globally, owing to its responsibility for numerous hospital acquired infections, also known as healthcare associated infections (HCAI) [1]. HCAI have led to extensive health and economic losses, while infections from multi-drug resistance (MDR) pathogenic bacteria and fungi strains remain progressively intractable. Consequently, consistent scientific pathways have been intensified to develop further solutions such as newly synthesized, either chemically or naturally derived, antimicrobial agents in order to substitute for those that developed resistance or to proceed via other newly discovered pathways [2,3]. However, the Infectious Disease Society of America (IDSA) has highlighted six major bacterial species ESKAPE pathogens (*Enterococcus faecium, Staphylococcus aureus, Klebsiella pneumonia, Acinetobacter baumannii, Pseudomonas aeruginosa* and *Enterobacter cloacae*) as being the utmost dangerous ones due to their patterns of antibiotic resistance and responsibility for many infections worldwide [4,5]. Nevertheless, invasive fungal diseases (exemplified by candidiasis that is caused by microscopic fungi candida albicans) have formed life-threatening conditions, especially for immune-compromised hosts (cancer, AIDS or organ transplantations). Moreover, further reported challenges have been encountered by scientists such as the variability detected in the treatment protocol outcomes due to subjective factors, resistance emergence, drug toxicity and pharmacodynamic/kinetic complications [6]. Lansterol 14α-demethylase (CYP51), a member of the superfamily of heme-containing cytochrome P450 enzymes and a principal constitutive and executive component of the fungal unit, has proved its positive clinical contribution in combating stubborn fungal infections through its interaction with the heterocyclic azole moieties of various antifungal agents, thus inhibiting essential ergosterol biosynthesis [7].

Literature reviews have always highlighted the prominent influence of the triazole moiety and its fused analogues as effective antimicrobial agents exemplified by itraconazole, voriconazole, and posaconazole. Also, fluconazole **I** (another triazole containing antifungal agent) has

Abbreviations: CO-ADD, The Community for Antimicrobial Drug Discovery; CYP51, cytochrome P450 subtype-51; SEM, standard error of the mean.

* Corresponding author at: Department of Medicinal Chemistry, Faculty of Pharmacy, Beni- Suef University, Beni-Suef 62514, Egypt.
E-mail address: noha.metri@pharm.bsu.edu.eg (N.H. Amin).

https://doi.org/10.1016/j.bioorg.2021.104841
Received 15 December 2020; Received in revised form 20 February 2021; Accepted 17 March 2021
Available online 22 March 2021

been widely used in clinical cases owing to its particular molecular structure, where N4 of 1,2,4-triazole ring has been coordinated to the heme iron of CYP51. This coordination mode has been considered as an important key feature for its antifungal activity [8,9].

On the other hand, the 1,2,4-triazolo[1,5-*a*]pyrimidine nucleus (a subtype of purine analogs) has displayed a wide range of biological activities. To name but a few of such activities, triazolopyrimidine derivatives exhibited prominent antimicrobial [10], antitumor [11] and even anti-inflammatory [12] activities. Although the aforementioned nucleus under concern constituted two heterocyclic moieties (a pyrimidine ring with a triazole one), yet each of them has proven its efficacy separately where promising scientific results have resulted from such moieties whether combined or individually [8,10,13,14]. However, combining them in the same framework has been presumed to result in a synergistic antimicrobial outcome. A rising example for this fruitful combination was essramycin **II,** the first 1,2,4-triazolo[1,5-*a*]pyrimidine antibiotic [10,15,16]. Essramycin **II,** that was isolated from the culture broth of marine *Streptomyces* species, has exhibited considerable antimicrobial activity against Gram-positive and Gram-negative (MIC = 2.0–8.0 μg/ mL) bacterial strains and more than 50% inhibition rate against 14 kinds of phytopathogenic fungi at 50 μg/mL for some of the essramycin alkaloid derivatives [10,15–19].

Similarly, combining thiosemicarbazide and azomethine moieties with a triazole or a triazolopyrimidine core have preceded successful pharmacophores as antimicrobial lead compounds [20–25]. 1,2,4-Triazole derivative **III** (bearing an azomethine moiety) showed a considerable antimicrobial activity against both Gram-positive (MRSA) and Gram-negative bacteria (*Escherichia coli, Klebsiella pneumonia, Acinetobacter baumanni and, Pseudomonas aeruginosa)* with MIC values = 0.5 μg/ mL and 0.25–1.0 μg/ mL, respectively. On the other hand, compound **IV** (a thiosemicarbazide moiety linked to a triazolopyrimidine core) was reported to show a considerable therapeutic activity against Gram-positive bacteria strains with an interesting DNA displacement activity (IC_{50} = 22 μg/mL) [10].

Furthermore, amides have always been considered as important functional groups for medicinal chemists, where the carboxaimde group prevailed in more than 25% of known drugs, not to mention its feasible conjugation with a triazole moiety to result in manifested antimicrobial activities [26–31]. Compound **V (**constituted an amide group linked to a 1,2,4 triazole moiety) exhibited pronounced antimicrobial activities against several bacterial strains, specifically *Staphylococcus aureus* and *Escherichia coli* (MIC = 3.75 μM/mL), if compared to ampicillin (54 and 46 μM/ml, respectively) [29], Fig. 1**.**

In view of all the above mentioned scientific literature data and as a continuation of recent ongoing research programs concerned with various heterocyclic nuclei [9,10,32], newly designed triazolopyrimidine derivatives were synthesized. The design scope of those new compounds was based on combining substituted amides, thiosemicarbazide or Schiff's base moieties with either 5-amino-1,2,4 triazole derivatives or cyclized 1,2,4-triazolo[1,5-*a*]pyrimidine analogues, where synergism and toxicity limitation were crucial expected goals, Fig. 1**.** The newly synthesized compounds were screened for their antimicrobial activity against five bacterial strains: Methicillin Resistant *S. aureus* (MRSA) (Gram positive), *E. coli, K. pneumoniae, A. baumannii* and *P. aeruginosa* (Gram negative) and two fungal strains: *C. albicans* and *C. neoformans* at CO-ADD (The Community for Antimicrobial Drug Discovery), followed by cytotoxicity screening against human embryonic kidney cell lines and hemolysis of human red blood cells for the most potent compounds to ensure acceptable safety margin. Furthermore, mechanistic studies were performed using lanosterol 14α-demethylase. Moreover, computational molecular docking, *in silico* ADME studies prediction and drug-like characters of the compounds were investigated, Fig. 1.

2. Results and discussions:

2.1. Chemistry

The synthesis pathways for the target compounds **6a-g, 7, 10a-c, 11, 12a,b, 13a-c** and **14a,b** were presented in schemes 1-3. The structures of the newly synthesized compounds were established on their elemental analyses and spectral data (**supplementary CHEMISTRY**). In scheme 1, the starting material 5-amino-1*H*-[1,2,4] triazole-3-carboxylic acid **3** was synthesized following a classical condensation reaction of aminoguanidine bicarbonate and oxalic acid. Esterification of the acid product **3** gave the corresponding 5-amino-1*H*- [1,2,4] triazole-3-carboxylate **4** [33]. Then, the reaction of the ester **4** with hydrazine hydrate gave the corresponding hydrazide **5**. Consequently,

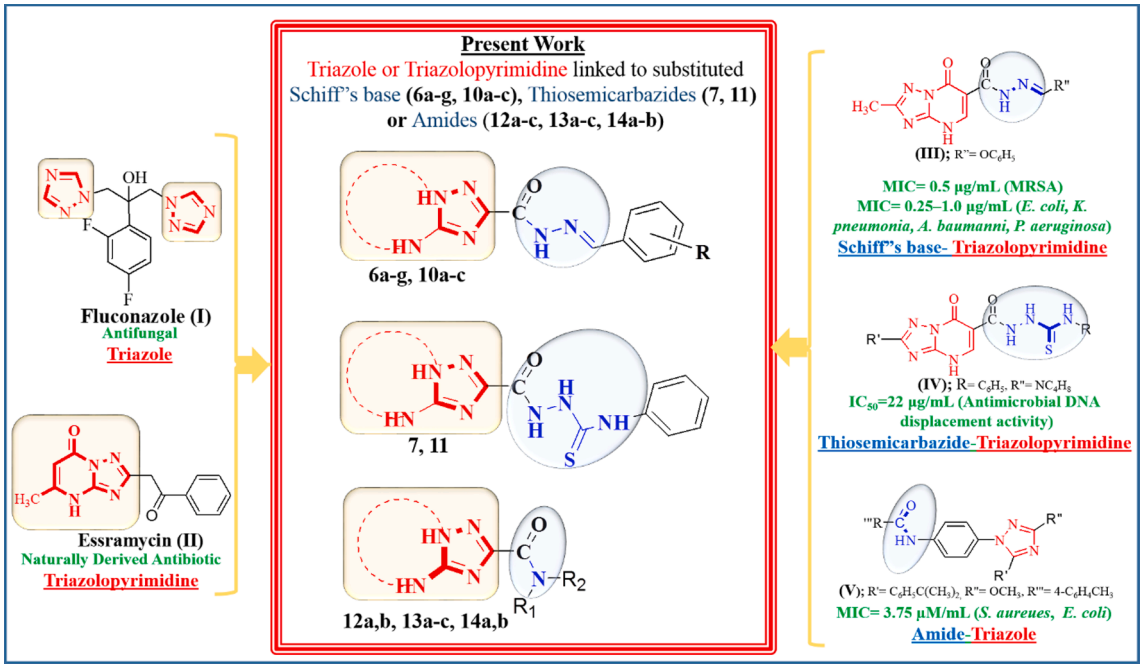

Fig. 1. Synthetic design strategy of the present target compounds **6a-g, 7, 10a-c, 11, 12a,b, 13a-c** and **14a,b.**

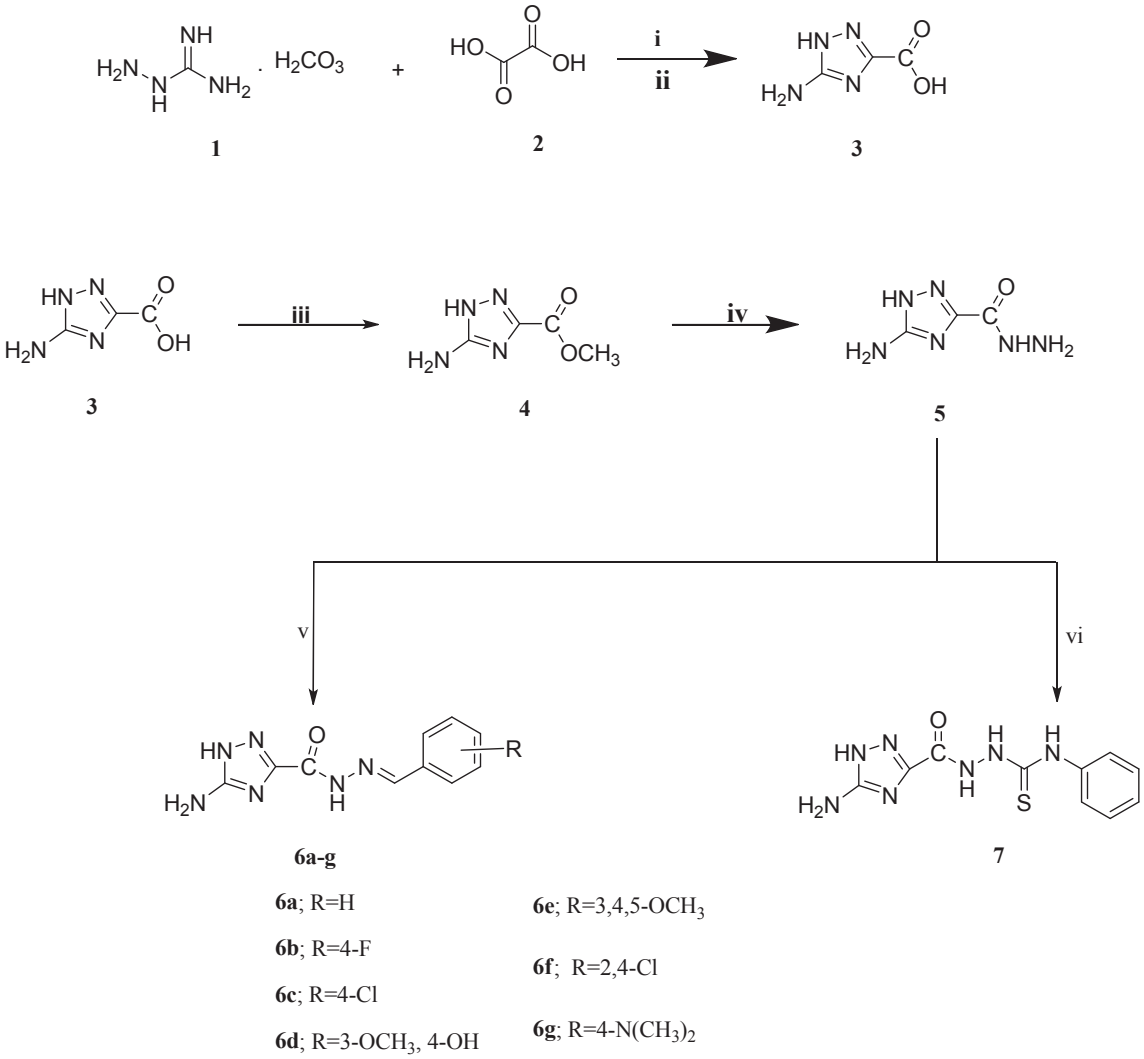

Scheme 1. Synthesis of compounds **1**–**7.**

the condensation reaction of compound **5** with different appropriate aromatic aldehydes (molar ratio 1:1) and in presence of an acidic catalyst afforded the corresponding hydrazones **6a-g.** On the other hand, the reaction of compound **5** with phenyl isothiocyanate resulted in *N*-phenyl thiosemicarbazide **7**. IR spectra of compounds **6a-g** were characterized by the disappearance of the forked peak of NH_2 attributed to the hydrazide moiety. Also, their ^{1}H NMR spectra showed singlet signals at $\delta = 8.34$–8.90 ppm and at 11.1–11.8 ppm (exchangeable with D_2O), attributed to N═C*H* and —CON*H* moieties of compounds **6a-g,** respectively**,** in addition to the characteristic signals of aromatic protons. Moreover, DEPT analysis was conducted for compound **6b** as a tool for its structural verification of the different carbon atoms types **(Supplementary DEPT)**, while ^{1}H NMR spectrum of compound **7** exhibited a singlet signal at $\delta = 9.88$ ppm (exchangeable with D_2O), attributed to the —CON*H* group, in addition to the characteristic signals of aromatic proton at $\delta = 7.13$–7.49 ppm.

As for scheme 2, cyclocondensation reaction of compound **4** with ethyl acetoacetate in glacial acetic acid gave the corresponding 1,2,4-triazolo[1,5-*a*]pyrimidine **8,** as reported [15]. Hydrazinolysis of the ester **8** with hydrazine hydrate gave the corresponding hydrazide **9** [15,17]. Furthermore, the condensation reaction of compound **9** with different appropriate aromatic aldehydes furnished the corresponding hydrazones **10a-c**. On the other hand, the reaction of compound **9** with phenyl isothiocyanate resulted in *N*-phenyl thiosemicarbazide **11**. IR spectra of compounds **10a-c** were characterized by the disappearance of the forked peak of NH_2, attributed to the hydrazide moiety and the corresponding appearance of a sharp single band, attributed to the endocyclic —*NH* group. Also, the ^{1}H NMR spectra showed the appearance of singlet signals at $\delta = 2.3$–2.34 ppm and at 5.85–5.89 ppm, attributed to the aliphatic CH_3 group and the aromatic proton of the pyrimidine ring, respectively. Similarly, ^{1}H NMR spectrum of compound **11** showed the appearance of singlet signals at $\delta = 2.30$ ppm and at 5.77 ppm, attributed to the aliphatic CH_3 and the aromatic proton of the pyrimidine ring. Further structure elucidation of the synthesized compounds **10b** and **11** using DEPT135 NMR spectra was performed to distinguish between different carbon atoms; CH_3, CH_2 and CH. **(Supplementary DEPT).**

Furthermore in scheme 3, nucleophilic substitution reactions for the amide compounds **12a,b** formation proceeded through the reaction of the ester derivative **4** with different appropriate aliphatic amines. On the other hand, the reaction of the ester **4** with aromatic amines, in presence of ammonium chloride, yielded the corresponding amides **13a-c.** Additionally, cyclization of compounds **13a,b** with ethyl acetoacetate (molar ratio 1:2) yielded the corresponding triazolo[1,5-*a*]pyrimidines **14a,b**. IR spectra of compounds **13a,b** revealed the disappearance of the band corresponding to the ester carbonyl group at 1722 cm^{-1} and the appearance of that corresponding to the amide group at 1640–1690 cm^{-1}. Also, their ^{1}H NMR spectra revealed a clear upgrade in the appearance of signals attributed to the aliphatic and aromatic protons of compounds **12a,b** and **13a-c,** respectively. Additionally, ^{1}H NMR

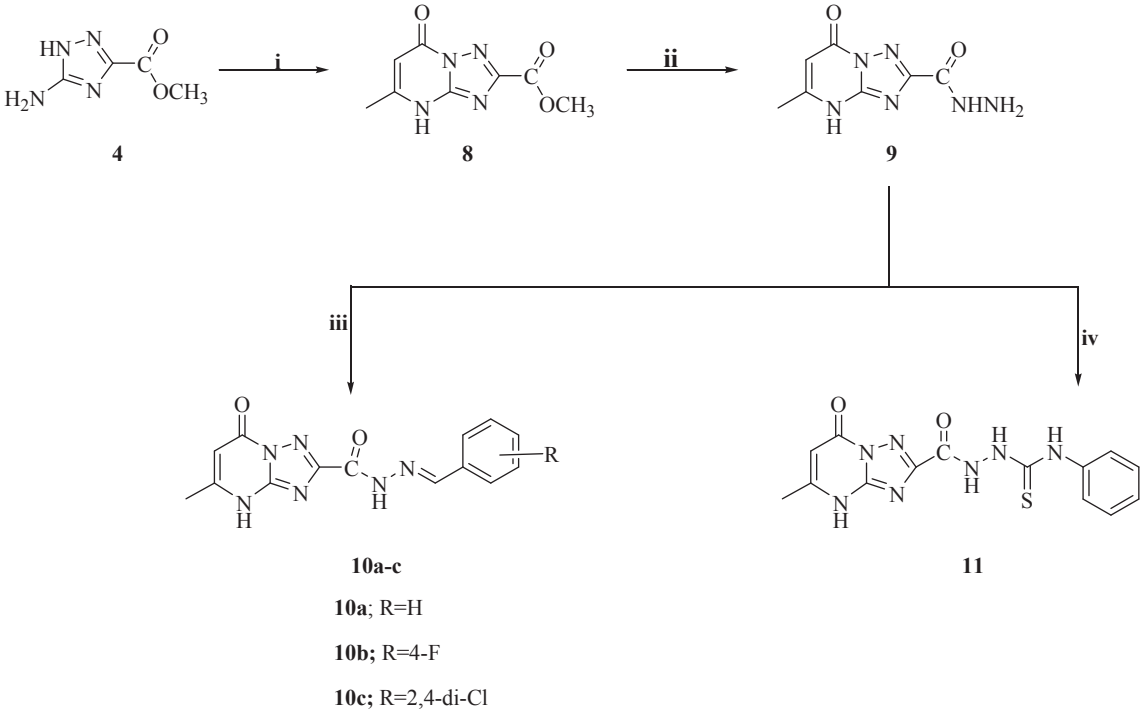

Scheme 2. Synthesis of compounds **8**–**11.**

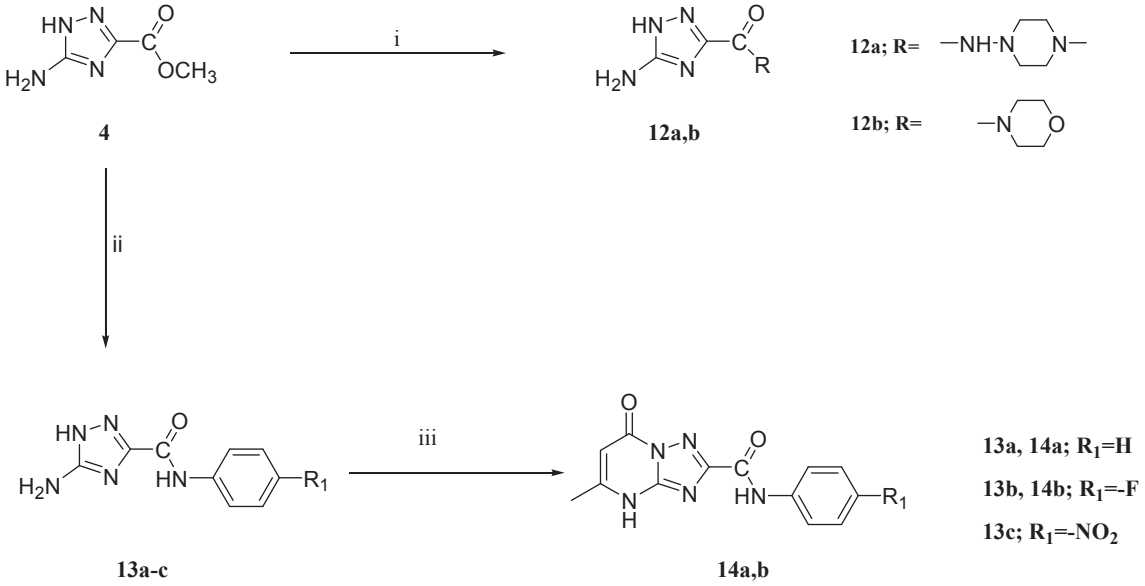

Scheme 3. Synthesis of compounds **12a,b, 13a-c and 14a-b.**

spectra of compounds **14a-c** showed the appearance of singlet signals at $\delta = 2.38$ ppm and at 5.96 ppm, attributed to the aliphatic CH_3 and the aromatic proton of the pyrimidine ring, respectively. Further structure elucidation of the synthesized compounds **13a, 13b, 14a** and **14b** using DEPT135 NMR spectra was performed to distinguish between different carbon atoms; CH_3, CH_2 and CH. **(Supplementary DEPT).**

Reagents and Conditions: i) Water, reflux, 6 h; **ii**) Aqueous KOH, reflux, 2 h; **iii**) MeOH, H_2SO_4, reflux, 24 h; **iv**) Hydrazine hydrate, EtOH, reflux, 7 h; **v)** Aromatic aldehydes, EtOH, AcOH, reflux, 4 h; **vi**) C_6H_5-NCS, EtOH, reflux, 3 h.

Reagents and Conditions: i) Ethylacetoacetate, AcOH, reflux, 6 h; **ii**) Hydrazine hydrate, EtOH, reflux, 4 h.; **iii**) Appropriate aromatic aldehydes, EtOH, AcOH, reflux, 4 h; **iv**) C_6H_5-NCS, EtOH, reflux, 3 h.

Reagents and Conditions: i) Appropriate aliphatic amines, TEA, reflux, 6 h. **ii)** Appropriate aromatic amines, NH_4Cl, reflux, 7 h; **iii)** Ethyl acetoacetate, AcOH, reflux, 7 h.

2.2. Biological evaluation

2.2.1. Antibacterial and antifungal activities

Antimicrobial screening for all the newly synthesized compounds was performed at CO-ADD (The Community for Antimicrobial Drug Discovery), funded by the Wellcome Trust (UK) and The University of Queensland, Australia **(Supplementary M1).** All compounds were

screened for their antibacterial activities at 32 μg/ml against five bacterial strains: Methicillin Resistant *S. aureus* (MRSA) (Gram positive), *E. coli, K. pneumoniae, A. baumannii* and *P. aeruginosa* (Gram negative) using ciprofloxacin as a positive control and for their antifungal activities against two fungal strains: *C. albicans* and *C. neoformans* using fluconazole as a positive control. Additionally, compounds displaying significant growth inhibition percentage (80–90%) were screened for their minimum inhibitory concentrations (MIC), where promising hits' minimum inhibitory concentrations (MIC) ranged from 4 to 32 μg/ ml, table 1. It was observed that all compounds showed weak antibacterial activity against the tested strains. On the other hand, compound **9** exhibited potent activity against *C. albicans* (MIC = 4 μg/ml). In addition, 5-amino-1*H*-1,2,4-triazole-3-carboxamides **13a** and **13b** showed moderate activities against *C. albicans,* expressed by a common (MIC = 32 μg/ml).

2.2.2. Cytotoxicity against human embryonic kidney cell line and hemolysis of human red blood cell effects

Screening for Cytotoxicity against human embryonic kidney cell line and hemolysis of human red blood cells was performed at CO-ADD institution **(Supplementary M1)** to ensure the safety margin for the potent compounds, as shown in table 1. Cytotoxicity of the samples were classified as toxic when their concentration at 50% cytotoxicity and HC_{10} concentration at 10% hemolysis exhibited values higher than 32 μg/mL.(CC_{50},$HC_{10} \leq$ 32 μg/mL). From the obtained results, the investigated compounds **9, 13a** and **13b** showed CC_{50} ˃ 32 μg/mL against the human embryonic kidney cell line and exhibited HC_{10} more than 32 μg/mL. 2.2.3. Lanosterol 14α-demethylase (CYP51) inhibition activity

Fluconazole is the most commonly used antifungal drug to inhibit lanosterol 14α-demethylase (CYP51) and ergosterol biosynthesis in the fungal cell membrane. The assay was performed at confirmatory diagnostic unit VACSERA, Egypt **(Supplementary M2),** using fluconazole as a reference standard drug with IC_{50} value = 0.25 μg/mL, as shown in table 2. The obtained results revealed that compound **9** possessed potent enzyme inhibitory activity with IC_{50} = 0.27 μg/mL, compared to 0.25 μg/mL of the reference drug fluconazole. On the other hand, compounds **13a** and **13b** showed moderate activities with IC_{50} = 0.46 and 0.32 μg/mL, respectively.

Table 2
Results of the molecular docking study of fluconazole and compounds **9, 13a** and **13b** into the active site of lansterol 14α-demethylase. (PDB ID: **1EA1**).

Compound	Energy score (S)	Bond length between Fe-Hem and Nitrogen atom	Interacting moiety of tested compounds	14α-demethylase assay IC_{50} (μg/mL)
9	−9.33	2.33	N_4	0.27
13a	−8.991	2.75	N_2	0.46
13b	−9.420	2.34	N_4	0.32
Fluconazole	−9.956	2.34	N_4	0.25

2.3. In-silico studies

2.3.1. Molecular docking

Molecular docking study was performed in an attempt to explain the enzymatic activity of the most active compounds (**9, 13a** and **13b),** based on the results of lansterol 14α- demethylase (CYP51) assay, through illustrating their positing and fitting into lansterol 14α- demethylase active binding site. Accordingly the three newly synthesized compounds were docked into the binding site of 14α- demethylase (PDB ID: **1EA1)** [34] to explore their potential binding modes compared to the co-crystalized ligand fluconazole **I.** The results were presented in table 2 and Figs. 2 and 3**.** The figures revealed similar binding modes for the studied compounds as those of the co-crystallized ligand, showing a coordination bond between N_4 and HEM. Moreover, the cyclized hydrazide compound **9** showed an additional coordination bond with HEM via its hydrazoide moiety, Fig. 3**.** This positioning supported the prominent *in- vivo* antifungal activity of the compound against Candida albicans fungal strains, in contrary to its substituted Schiff's bases **(10a-c)** or amide analogues **(14a,b),** figure S1 **(Supplementary FIGURES**). On the other hand, the schiff's base derivatives **(6a-g)** showed different

Table 1
The antimicrobial activities (growth inhibition % at 32 μg/mL concentration, MIC, cytotoxicity and hemolysis) of the examined compounds.

Code	Gram positive bacteria	Gram negative bacteria		Fungi					Cytotoxicity and hemolysis	
	MRSA [a]	*Ec* [b]	*Kp* [c]	*Ab* [d]	*Pa* [e]	*Ca* [f]		*Cn* [g]	CC_{50} (μg/mL)[d]	HC_{10} (μg/mL)[e]
	GI%[h]	GI%	GI%	GI%	GI%	GI%	MIC	GI%		
3	18.01	16.54	27.49	8.49	8.07	6.56	NT[i]	7.63	NT	NT
4	18.66	22.04	25.79	10.74	34.17	18.46	NT	6.86	NT	NT
5	15.47	12.65	23.62	6.54	16.09	7.11	NT	8.79	NT	NT
6a	7.31	13.47	14.08	8.49	25.87	3.67	NT	−4.29	NT	NT
6b	16.21	14.76	23.75	1.89	19.59	3.33	NT	7.08	NT	NT
6c	5.6	10.46	9.29	7.97	13.21	3.88	NT	−14.37	NT	NT
6d	9.57	16.94	15.19	1.12	22.49	3.67	NT	−5.36	NT	NT
6e	8.32	16.02	20.5	5.9	14.76	6.91	NT	−3.21	NT	NT
6f	9.06	12.93	17.28	7.65	16.13	12.62	NT	−4.93	NT	NT
6g	7.21	18.07	22.91	3.25	36.93	5.81	NT	1.2	NT	NT
7	13.59	40.1	37.42	37.4	43.04	5.67	NT	4.72	NT	NT
8	16.7	−0.46	6.01	13.95	6.63	2.13	NT	−7.64	NT	NT
9	16.09	65.56	12.72	8.29	17.93	**84.29**	4	−5.94	**>32**	**>32**
10a	15.82	1.52	9.02	8.71	10.32	2.49	NT	−5.43	NT	NT
10b	13.64	3.48	10.14	10.95	10.55	4.22	NT	−7.64	NT	NT
10c	11.62	12.83	7.23	8.49	6.21	7.4	NT	−6.74	NT	NT
11	12.49	33.45	12.74	2.08	2.92	3.43	NT	−0.34	NT	NT
12a	7.31	17.31	20.85	4.12	16.34	34.55	NT	−3.21	NT	NT
12b	3.67	16.21	21.95	4.85	23.63	25.68	NT	2.01	NT	NT
13a	9.77	13.72	19.96	4.71	8.19	**83.99**	**32**	4.93	**>32**	**>32**
13b	4.97	16.47	23.09	5.45	12.64	**88.92**	**32**	−2.41	**>32**	**>32**
13c	15.39	10.87	23.04	14.46	8.55	4.98	NT	−5.79	NT	NT
14a	17.26	−8.4	8.52	6.06	4.27	7.69	NT	−6.45	NT	NT
14b	14.02	−5.32	5.4	13.18	5.75	2.78	NT	−3.76	NT	NT
Flu-conazole	–	–	–	–	–	–	0.125	–	–	–
Cipro-floxacin	0.25	0.007	0.5	1	0.25	–	–	–	–	–

[a]Methicillin Resistant *S.* aureus, [b]E. coli, [c]K. pneumonia, [d]A. baumannii, [e]P. aeruginosa, [f]C. albicans, [g]C. neoforma, [h]growth inhibition %, [i]not tested.

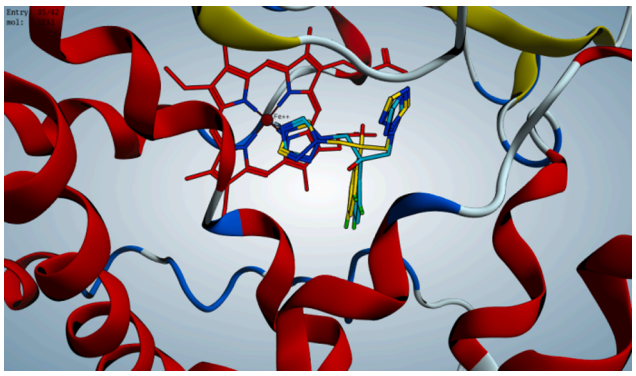

Fig. 2. Superimposition of the co-crystallized ligand, fluconazole (Yellow) and re-docked ligand (Turquoise). (For interpretation of the references to colour in this figure legend, the reader is referred to the web version of this article.)

disposition and interaction modes, a case that supported their weak *in-vitro* antimicrobial activities against the tested strains. Also, the amides (**12a,b** and **13a-c)** showed weak antibacterial and moderate antifungal activities against the tested strains, where the fluorinated phenyl carboxamide **(13b)** was bound to HEM more effectively than its unsubstituted analogue (**13a**), **figure 3 and S1 (Supplementary FIGURES).** Moreover, the validity of the docking protocol was ensured via re-docking of the co-crystallized fluconazole into the active site. Docking results obtained were presented in Fig. 2**,** which showed a near perfect alignment with the original ligand as obtained from the X-ray resolved PDB file. The re-docked ligand showed rmsd of 0.8 between the docked pose and the co-crystallized ligand (energy score (S) = −9.956 kcal/mol), and by the ability of the docking poses to reproduce the key interactions accomplished by the co-crystallized ligand with HEM B460.

2.3.2. Computational analysis: In-silico prediction of physicochemical properties, pharmacokinetics and drug-likeness profile

In-silico ADMET prediction studies have played an increasingly important part in drug research and development through providing an effective way to assess multiple pharmacokinetic properties in hit-to-lead and lead-optimization campaigns. The importance of such a strategy alongside the evolution of chemoinformatics has grown since the 1960 s, not to mention the widely applied drug-likeness concepts of the 1990 s. Accordingly, predicted absorption, distribution, metabolism and excretion (ADME) studies were performed for the most active compounds (**9, 13a** and **13b)** and results were presented in tables 3-5. Herein, pre-ADME [35,36]**,** molinspiration [37,38], Molsoft [39] and Swiss ADME [40–42] were the software used to predict the aforementioned pharmacokinetic parameters of the most active compounds. The SMILE molecular structures of the compounds were obtained from PubChem (https://pubchem.ncbi.nlm.nih.gov). The performed *in-silico* studies were used as a predictive tool to investigate the expected pharmacokinetic properties of the target compounds to improve their *in- vivo* outcomes through a pharmacokinetic-pharmacodynamic balance [35–42].

Literature reports have proved that compounds were most likely to have poor absorption for various reasons, such as having a molecular weight (MW) ˃ 500, a calculated octanol/water partition coefficient logP ˃ 5, number of H-bond donors ˃ 5 or the number of H-bond acceptors ˃10. Also, assessing other parameters has been helpful as virtual screening tools, such as calculating the partition coefficient (a descriptive parameter for the lipophilicity of a drug) and topological polar surface area PSA (a criteria that allows the prediction of transport properties of polar atoms through membranes). Moreover, the number of rotatable bonds (NROTB) has been an important descriptor, associated with any single non-ring bond, bounded to nonterminal heavy (i.e., non-hydrogen) atom, where a large number of rotatable bonds (≥10) indicated poor oral bioavailability. Herein, molinspiration [37,38] and Swiss ADME [40–42] were the software used to predict the aforementioned pharmacokinetics parameters of the most active compounds, as shown in table 3. The investigated compounds were satisfying to Lipinski's rule of five, where the molecular weight ranged from 203 to 221 (<500), logP values ranged from −0.77 to 0.76 (<5); hydrogen bond donors were 3 (<5) and finally hydrogen bond acceptors ranged from 3 to 5 (<10). Theoretically speaking, such results would result in compounds with anticipated good oral absorption. Also, the compounds exhibited NROTB range from 2 to 3 (<10) and PSA range from 96.69 to 118.17 (<140A^2), indicating good cell permeability through various biological membranes.

Additionally, further ADME parameters were evaluated such as the drug solubility S (a key parameter determining dissolution rate to achieve desired oral bioavailability) and the drug likeness score, which described compounds with desirable bioavailability during the early phases of drug discovery (larger score values tended to be for particular molecules of higher activity). Herein, Molsoft [39] and SwissADME [40–42] software were applied to predict drug likeness model scores and solubility of the compounds, as shown in Table 4. Absorption and distribution characteristics have been known to be changed by aqueous solubility (solubility improves when solubility values are more than 0.0001 mg/mL). The tested compounds showed values ranging from 1.08 to 1.91 mg/mL, thus promising solubility characteristics have been expected. Also, the more positive drug likeness score values, the more likely the compound was expected to be as a promising therapeutic pharmacophore. A positive model score was attributed for compounds **9** and **13b** (0.45 and 0.95, respectively), in contrast to compound **13a,** which showed a negative value (−0.07). In addition, all the compounds were found to be orally safe (less than 1 violation of the Lipinski's rule of five) and thus they could be anticipated to possess good oral bioavailability and cell permeability.

Furthermore, a pre-ADMET software was applied to estimate the various ADMET factors that might affect the pharmacokinetics of the synthesized compounds, exemplified by the blood brain barrier partition coefficient BBB (a key parameter for brain therapeutically active targeted drugs), the Caco2 (human colon adenocarcinoma) permeability coefficient (a human colon epithelial cancer cell line that differentiates to form tight junctions between cells to serve as a model of paracellular movement of compounds across the monolayer), the human intestinal absorption HIA (one of the key processes determining factors of the drug bioavailability upon oral administration as there is a correlation between the structures of organic compounds and their human small intestinal absorption and the human plasma protein binding PPB (an essential criteria to estimate the fraction of drug bound to plasma proteins and thus may predict the efficiency of the free drug that can cross various biological membranes and thus can bind to the intended molecular target). Last but not least, inhibition of cytochrome P4502D6 (CYP4502DC) and Madin-Darby canine kidney cells MDCK permeability coefficient provided helpful *in vitro* tools to assess a drug's permeability and transporter interactions during drug discovery and development. Herein, ADME data of the most active compounds was calculated using preADMET software [35,36]**,** as shown in table 5**.** All the investigated compounds showed a medium CNS absorption range from 0.132 to 0199, comparable to the normal medium range ≤ 0.1–2. Also the tested compounds showed medium permeability in Caco2 model range from 4.3 to 18.9 nm/s (normal range 4–70 nm/s), in addition to high permeability in MDCK model, ranging from 2.35 to 220.6 nm/s (normal range 4–70 nm/s). Moreover, the compounds showed no inhibition of CYP2D6 enzyme and thus no interaction with CYP2D6 inducers or inhibitors. Last but not least, the tested compounds showed moderate absorption, ranging from 60.3 to 71.2% (normal range 30–70 %) and low plasma protein binding, ranging from 9.4 to 23.9 (normal range ≤ 90).

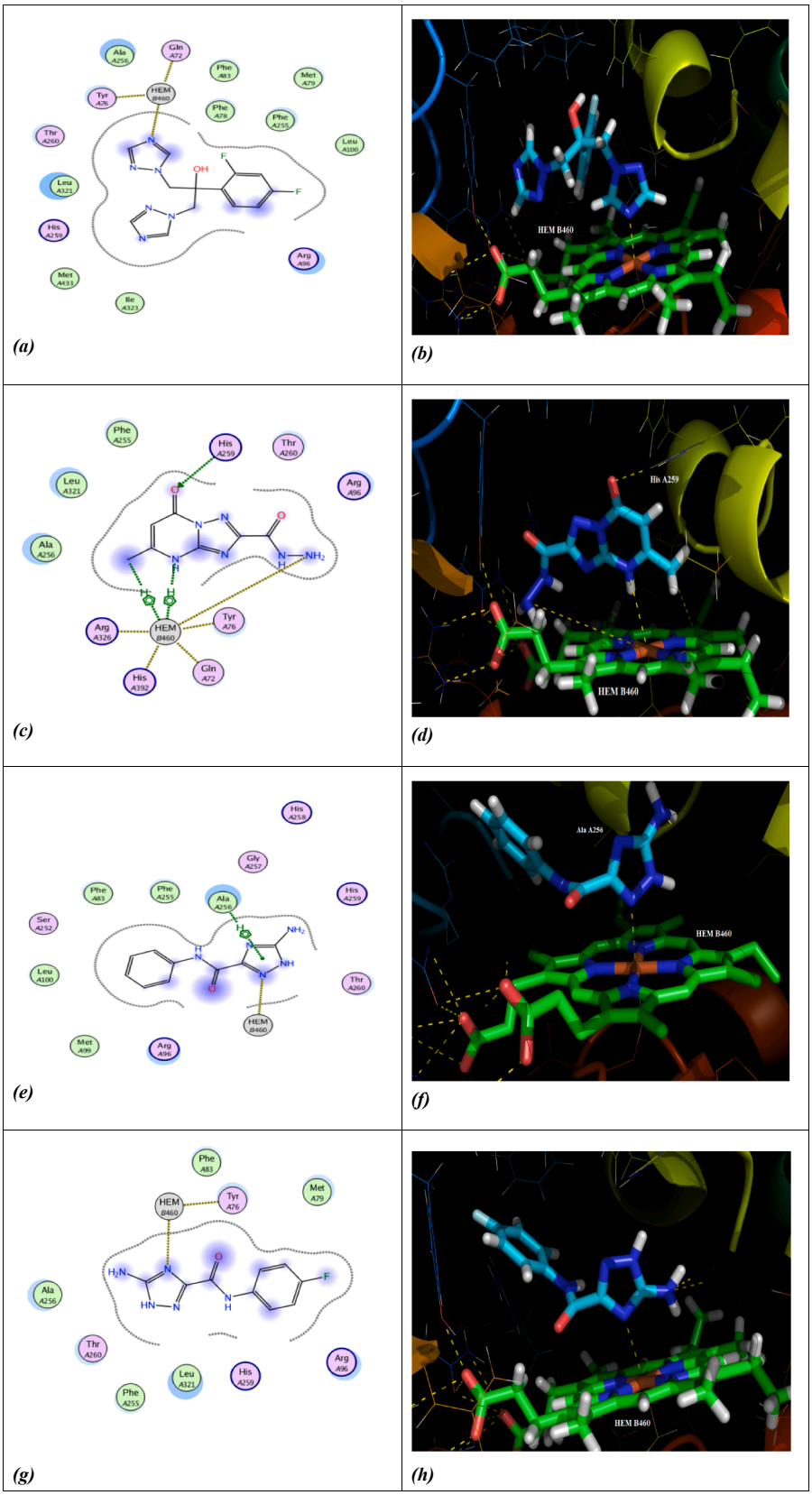

Fig. 3. 2D and 3D interaction diagrams of fluconazole ***(a)*** and ***(b),*** compound **9** ***(c)*** and ***(d),*** compound **13a** ***(e)*** and ***(f)*** and compound **13b** ***(g)*** and ***(h)***, respectively, with 14-α demethylase (PDB: **1EA1**).

Table 3
Estimated physicochemical properties of compounds **9, 13a** and **13b** using SwissADME & Molinspiration software.

Physicochemical properties					log P	Code
TPSA[c] (A^2)	H-bond donor	H-bond acceptor	NORTB[b]	MW[a]		
118.17	3	5	2	208.18	−0.77	**9**
96.7	3	3	3	203.2	0.43	**13a**
96.69	3	4	3	221.19	0.76	**13b**

[a]**MW**, molecular weight; [b]NROTB, number of rotatable bonds [c]**TPSA**, topological polar surface area.

Table 4
Predicted drug likeness using Molsoft & SwissADME software.

Code	Solubility (mg/L)	Drug likeness model score	Lipinski's rule violations	Bioavailability score
9	1.08	0.45	0	0.55
13a	1.91	−0.07	0	0.55
13b	1.09	0.94	0	0.55

Table 5
ADME data of most active compounds calculated using preADMET software.

Code	Pharmacokinetics					
	BBB[a]	**Caco-2**[b] (nm/s)	**HIA**[c] **(%)**	**MDCK**[d] (nm/s)	**PPB**[e]	**CYP 2D6**[f]
9	0.132	4.3	60.3	2.35	9.4	No
13a	0.177	7.02	71.2	220.6	23.9	No
13b	0.199	18.9	71.1	81.0	23.4	No

[a]**BBB:**blood brain barrier penetration; [b]**CACO-2:** permeability through cells derived from human colon adenocarcinoma; [c]**HIA:** percentage human intestinal absorption; [d]**MDCK:** permeability through Madin-Darby canine kidney cells; [e]**PPB:** plasma protein binding; [f]**CYP2D6:** cytochrome P450 2D6.

3. Conclusion

A novel series of 5-amino-1,2,4 triazole derivatives and their cyclized 1,2,4-triazolo[1,5-*a*]pyrimidine analogues, were designed, synthesized and their structures were characterized by melting points, IR, ^{1}H NMR, ^{13}C NMR, DEPT ^{135}, elemental analyses and mass spectroscopy. The antimicrobial activities of all the compounds were evaluated against five bacterial strains (Methicillin Resistant *S. aureus* (MRSA), *E. coli, K. pneumoniae, A. baumannii* and *P. aeruginosa)* using ciprofloxacin as a positive control and against two fungal strains (*C. albicans* and *C. neoformans*) using fluconazole and amphotericin B as positive controls at CO-ADD, Australia. Compounds **9, 13a** and **13b** showed promising anti-*candida albicans* activities (MIC values = 4–32 μg/ml), associated with significant safety profiles against certain cytotoxic parameters. They were not cytotoxic against neither human embryonic kidney cell line nor 10% red blood cell hemolysis, at concentrations up to 32 μg/mL. Further mechanistic studies highlighted the interesting potency of the hit hydrazide derivative **9** due to its considerable ability of lanosterol 14α-demethylase (CYP51) inhibition (IC_{50} value = 0.27 μg/mL), compared to fluconazole (IC_{50} = 0.25 μg/mL). Additionally, *in-silico* docking studies showed similarity in the binding patterns of X-ray structures of both the synthesized compounds (**9, 13a** and **13b)** and fluconazole, targeting the same pocket of lanosterol 14-α- demethylase (CYP51) active site (1EA1). Finally, *in silico* prediction of physicochemical properties, pharmacokinetics and drug-likeness profile studies of the most active compounds showed favorable oral bioavailability, cell permeability and minimal toxicity. Collectively, compounds **9**, **13a** and **13b** showed coinciding and promising *in- vivo*, *in- vitro* and *in-silico* results. Accordingly, the aforementioned compounds, topped by compound **9,** could be considered as reliable pharmacophores for further screening in order to generate efficient antifungal agents with considerable safety profiles.

4. Experimental

4.1. Chemistry

Chemical reagents and solvents were all obtained from Sigma Aldrich, Germany. Reactions were monitored by TLC: Pre-coated plastic sheets, 0.2 mm silica gel with fluorescent indicator (E. Merck). Melting points were determined on Stuart electrothermal melting point apparatus and were uncorrected. IR spectra were recorded as KBr disks on a Bruker spectrophotometer (Karlsruhe, Germany) at Nahda University, Beni-Suef, Egypt. ^{1}H NMR spectra were carried out on Bruker apparatus 400 MHz (Karlsruhe, Germany) at Sohag University, Sohag, Egypt, using TMS as internal reference, chemical shifts (values are given in parts per million (ppm) using DMSO-d_6 or $CDCl_3$ as solvents. ^{13}C NMR and DEPT 135 were recorded using Bruker 100 MHz NMR, using TMS as internal standard and chemical shifts were recorded in ppm on δ scale (Karlsruhe, Germany) at Sohag University,Sohag, Egypt. Elemental analyses (C, H and N) and mass spectrometry were performed on FLASH 2000 CHNS/O analyser, VARIO-Elementer apparatus at The Regional Center for Mycology and Biotechonology, Al-Azhar University, Cairo, Egypt. Compounds **3**, **4** [33]**, 5, 13a** [26] and **8**, **9** [15,17] were prepared according to their reported procedures.

4.1.1. General procedure for the synthesis of compounds *6a-g*

A mixture of compound **5** (0.0017 mol), appropriate aldehyde (0.0017 mol) and catalytic glacial acetic acid (1 mL) in absolute ethanol (20 mL) was heated under reflux for 4 h. The reaction was monitored by TLC; then the obtained precipitate from the hot ethanolic solution was filtered and re-crystallized from ethanol to offer products **6a-g**.

*4.1.1.1. 5- Amino-N′-benzylidene-1H-1,2,4-triazole-3-carbohydrazide **6a**.* White powder, yield: 55.6%, m.p.: 265–267 °C; FT-IR (KBr (υ_{max}/ cm^{-1}): 3220 (forked NH_2), 3307 (NH), 1692 (C═O amide), 3047 (CH aromatic); ^{1}H NMR (DMSO-d_6, 400 MHz) δ = 6.06 (s, 2H, NH_2), δ = 7.45–7.70 (m, 5H, Ar-H), 8.51 (s, 1H, —N═C*H*), 11.41 (s, 1H, —CON*H*—, D_2O exchangeable), 12.49 (s, 1H, cyclic —NH—, D_2O exchangeable); EIMS *m/z* (%): 230.98 [M^+] (31.26), 208.17 (100); Elemental analysis calculated for $C_{10}H_{10}N_6O$ (230.23): C, 52.17; H, 4.38; N, 36.50; Found C, 52.31; H, 4.52; N, 36.73.

*4.1.1.2. 5- amino -N′-(4-fluorobenzylidene)-1H-1,2,4-triazole-3-carbohydrazide **6b**.* White powder, yield: 60.4%, m.p.: 241–243 °C; FT-IR (KBr (υmax/ cm-^{1}): 3273 (forked NH_2), 3440 (NH), 1687 (C═O amide), 3035 (CH aromatic); ^{1}H NMR (DMSO-d_6, 400 MHz) δ = 6.08 (s, 2H, NH_2), 7.50, 7.52 (d, J = 8.00 Hz, 2H, Ar-H), 7.70, 7.72 (d, J = 8.00 Hz, 2H, Ar-H), 8.50 (s, 1H, —N═C*H*), 11.48 (s, 1H, —CON*H*—, D_2O exch.) 12.50 (s, 1H, cyclic —NH—, D_2O exchangeable); ^{13}C NMR (DMSO-d_6):(100 MHz) δ = 116.19, 116.41, 129.62, 129.70, 131.53, 147.34, 152.35, 164.80; DEPT C^{135} ($CDCl_3$, 100 MHz, δ ppm); 116.27 (phenyl CH-3 + CH-5), 116.49 (phenyl CH-2 + CH-6), 147.19 (—N═CH);); EIMS *m/z* (%): 248.79 [M^+] (27.51), 206.82 (100); Elemental analysis calculated for $C_{10}H_9FN_6O$ (248.22): C, 48.39; H, 3.65; N, 33.86; Found C,48.59; H,3.75;N,33.68.

*4.1.1.3. 5- Amino-N′-(4-chlorobenzylidene)-1H-1,2,4-triazole-3-carbohydrazide **6c**.* White powder, yield: 55.9%, m.p.: 236–238 °C; FT-IR (KBr (υmax/ cm-1): 3267 (forked NH2), 3325 (NH), 1692 (C═O amide), 3050 (CH aromatic); ^{1}H NMR (DMSO-d_6, 400 MHz) δ = 6.04 (s, 2H, NH_2), 7.22, 7.24 (d, J = 8.00 Hz, 2H, Ar-H), 7.54, 7.56 (d, J = 8.00 Hz, 2H, Ar-H), 8.44 (s, 1H, —N═C*H*), 11.36 (s, 1H, —CON*H*—, D_2O exchangeable), 12.42 (s, 1H, cyclic —NH—, D_2O exchangeable); EIMS *m/z* (%): 263.08 [M^+−H] (79.20), 266.10 [M+2] (27.50), 266.76

[M+2] (45.45), 188.07 (100); Elemental analysis calculated for $C_{10}H_9ClN_6O$ (264.67) C, 45.38; H, 13.40; N, 31.75; Found C, 45.49; H, 3.51; N, 31.91.

4.1.1.4. 5-Amino-N′-(4-hydroxy-3-methoxybenzylidene)-1H-1,2,4-triazole-3-carbohydrazide ***6d.*** White powder, yield: 29.6%, m.p.: 275–277 °C; FT-IR (KBr (υ_{max}/ cm^{-1}): 3445 (forked NH_2), 3319 (NH), 1674 (C═O amide), 3070 (CH aromatic); ^{1}H NMR (DMSO-d_6, 400 MHz) δ = 3.84 (s, 3H, OCH_3), 6.06 (s, 2H, NH_2), 6.83, 6.85 (d, J = 8.00 Hz, 1H, Ar-H), 7.05, 7.07 (d, J = 8.00 Hz, 1H, Ar-H), 7.30 (s, 1H, Ar-H), 8.37 (s, 1H, —N═C*H*), 9.36 (s, 1H, phenolic OH, D_2O exchangeable), 11.18 (s, 1H, —CON*H*—, D_2O exchangeable), 12.46 (s, 1H, cyclic —NH—, D_2O exchangeable); ^{13}C NMR (DMSO-d_6):(100 MHz) δ = 56.19, 109.88, 116.00, 122.52, 123.33, 126.63, 148.56, 148.99, 149.49, 157.54, 163.22; EIMS *m/z* (%): 276.60 [M^+] (21.83), 107.36 (100); Elemental analysis calculated for $C_{11}H_{12}N_6O_3$ (276.25) C, 47.83; H, 4.38; N, 30.42; Found C,47.59; H,4.52;N,30.25.

4.1.1.5. 5-Amino-N′-(3,4,5-trimethoxybenzylidene)-1H-1,2,4-triazole-3-carbohydrazide ***6e.*** White powder, yield: 88.6%, m.p.: 232–234 °C; FT-IR (KBr (υ_{max}/ cm^{-1}): 3439.73 (forked NH_2), 3320 (NH), 1662 (C═O amide), 3050 (CH aromatic); ^{1}H NMR (DMSO-d_6, 400 MHz) δ = 3.74 (s, 3H, OCH_3), 3.85 (s, 6H, OCH_3) 6.06 (s, 2H, NH_2), 6.99, (s, 2H, Ar-H), 8.42 (s, 1H, —N═C*H*), 11.37 (s, 1H, —CON*H*—, D_2O exchangeable), 12.50 (s, 1H, cyclic —NH—, D_2O exchangeable); ^{13}C NMR (DMSO-d_6): (100 MHz) δ = 56.56, 60.61, 105.06, 130.38, 140.01, 144.35, 148.48, 153.70, 156.34, 161.31; EIMS *m/z* (%): 230.27 [M^+] (29.13), 215.97 (100); Elemental analysis calculated for $C_{13}H_{16}N_6O_4$ (320.12) C, 48.75; H, 5.03; N, 26.24; Found C, 48.96; H, 5.24; N, 26.45.

4.1.1.6. 5- Amino-N′-(2,4-dichlorobenzylidene)-1H-1,2,4-triazole-3-carbohydrazide ***6f.*** White powder, yield: 85.4%, m.p.: 215–217 °C; FT-IR (KBr (υ_{max}/ cm^{-1}): 3330 (forked NH_2), 3426 (NH), 1672 (C═O amide), 3029 (CH aromatic); ^{1}H NMR (DMSO-d_6, 400 MHz) δ = 6.08 (s, 2H, NH_2), 7.49, 7.51 (d, J = 8.00, 1H, Ar-H), 7.67 (s, 1H, Ar-H), 8.00, 8.02 (d, J = 8.00, 1H, Ar-H), 8.90 (s, 1H, —N═C*H*), 11.88 (s, 1H,—CON*H*—, D_2O exchangeable), 12.53 (s, 1H, cyclic —NH—, D_2O exchangeable); EIMS *m/z* (%): 298.33 [M^+] (14.54), 302.65 (4.76), 303.28 (14.54), 251.87 (100); Elemental analysis calculated for $C_{10}H_8Cl_2N_6O$ (299.12) C, 40.15; H, 2.70; N, 28.10; Found C, 40.33; H, 2.92; N, 28.31.

4.1.1.7. 5-Amino-N′-(4-(dimethylamino)benzylidene)-1H-1,2,4-triazole-3-carbohydrazide ***6 g.*** Yellow powder, yield: 70.8%, m.p.: 246–248 °C; FT-IR (KBr (υ_{max}/ cm^{-1}): 3320 (forked NH_2), 3331 (NH), 1689 (C═O amide), 3040 (CH aromatic); ^{1}H NMR (DMSO-d_6, 400 MHz) δ = 2.98 (s, 6H, CH_3), 6.05 (s, 2H, NH_2), 6.75, 6.77 (d, J = 8.00, 2H, Ar-H), 7.50, 7.52 (d, J = 8.00, 2H, Ar-H), 8.34 (s, 1H, —N═C*H*), 11.04 (s, 1H, —CON*H*—, D_2O exchangeable), 12.44 (s, 1H, cyclic —NH—, D_2O exchangeable); EIMS *m/z* (%): 273.69 [M^+] (45.79), 174.79 (100); Elemental analysis calculated for $C_{12}H_{15}N_7O$ (273.29) C, 52.74; H, 5.53; N, 35.88; Found C,52.51;H,5.39;N,35.68.

4.1.2. Synthesis of 2-(5-amino-1H-1,2,4-triazole-3-carbonyl)-N-phenylhydrazinecarbothioamide ***7***

Phenyl isothiocynate (0.002 mol) was added to a solution of compound **5** (0.002 mol) in absolute ethanol (20 mL) and heated under reflux for 3 h. The reaction mixture was concentrated under reduced pressure; the product was collected and re-crystallized from ethanol to give the corresponding compound **7**.

White powder, yield 88%, m.p.: 288–290 °C FT-IR (KBr (υ_{max}/ cm^{-1}): 3447 (forked NH_2), 3367 (—NH—), 1681 (C═O amide), 3020 (CH aromatic); ^{1}H NMR (DMSO-d_6, 400 MHz) δ = 4.16 (s, 1H, —NH—, D_2O exchangeable), 5.33 (s, 1H, —NH—, D_2O exchangeable), 6.43 (s,2H,NH_2, D_2O exchangeable), 7.13–7.49 (m, 5H, Ar-H), 9.88 (s, 1*H*, —NH—, D_2O exchangeable), 12.49 (s, 1H, cyclic —NH—, D_2O exchangeable); EIMS *m/z* (%): 277.98 [M^+] (31.31), 82.23 (100); Elemental analysis calculated for C10H11N7OS (277.31) C, 43.31; H, 4.00; N, 35.36; Found C,43.41;H,4.3;N,35.48.

4.1.3. General procedure for the synthesis of compounds ***10a-c***

A mixture of compound **9** (0.00072 mol), appropriate aldehyde (0.00076 mol) and catalytic glacial acetic acid (1 mL) in absolute ethanol (20 mL) was heated under reflux for 4 h. The reaction was monitored by TLC; then the obtained precipitate from the hot ethanolic solution was filtered and re-crystallized from ethanol to offer products **10a-c**.

4.1.3.1. Benzylidene-5-methyl-7-oxo-4,7-dihydro-[1,2,4]triazolo[1,5-a] pyrimidine-2-carbohydrazide ***10a.*** White powder, yield 62.5%, m.p.: 184–186 °C FT-IR (KBr (υ_{max}/ cm^{-1}): 3273–3193 (NH pyrimidine, NH hydrazone), 1667 (C═O amide), 3020 (CH aromatic); ^{1}H NMR (DMSO-d_6, 400 MHz) δ = 2.33 (s, 3H, —CH_3—), 5.88 (s, 1H, Ar-H), 7.18–7.95 (m, 5H, Ar-H), 8.49 (s, 1*H*, —N═C*H*—), 10.84 (s, 1H, cyclic —NH—, D_2O exchangeable), 11.90 (s, 1H, —NH—, D_2O exchangeable); EIMS *m/z* (%): 296.10 [M^+] (42.43), 203.86 (100); Elemental analysis calculated for $C_{14}H_{12}N_6O_2$ (296.28) C, 56.75; H, 4.08; N, 28.36; Found C,56.73; H,4.06; N,28.34.

4.1.3.2. (4-Fluorobenzylidene)-5-methyl-7-oxo-4,7-dihydro-[1,2,4]triazolo[1,5-a]pyrimidine-2-carbohydrazide ***10b.*** White powder, yield 85%, m.p.: 174–176 °C FT-IR (KBr (υ_{max}/ cm^{-1}): 3312–3258 (NH pyrimidine, NH hydrazone), 1681 (C═O amide), 3019 (CH aromatic); ^{1}H NMR (DMSO-d_6, 400 MHz) δ═2.3 (s, 3H, —CH_3—), 5.89 (s, 1H, Ar-H), 7.33,7.35 (d, J = 8.00 Hz, 2H, Ar-H), 7.80, 7.82 (d, J = 8.00 Hz, 2H, Ar-H), 8.61 (s, 1*H*, —N═C*H*—), 10.00 (s, 1H, cyclic —NH—, D_2O exchangeable), 12.25 (s, 1H, —NH—, D_2O exchangeable); ^{13}C NMR (DMSO-d_6):(100 MHz) δ = 19.55, 99.11, 115.73, 129.99, 131.25, 148.77, 151.48, 155.91, 156.02, 164.96; DEPT C^{135} ($CDCl_3$, 100 MHz, δ ppm); 19.82 (pyrimidine C*H*$_3$-5), 98.96 (pyrimidine C*H*-6), 116.35 (phenyl C*H*-3 + C*H*-5), 116.57 (phenyl C*H*-2 + C*H*-6), 148.66 (—N═C*H*); EIMS *m/z* (%): 314.58 [M^+] (31.52), 269.50 (100); Elemental analysis calculated for $C_{14}H_{11}FN_6O_2$ (314.27) C, 53.50.34; H, 3.53; N, 26.74; Found C, 53.49; H,3.50; N,26.73.

4.1.3.3. (2,4-Dichlorobenzylidene)-5-methyl-7-oxo-4,7-dihydro-[1,2,4] triazolo[1,5-a] pyrimidine-2-carbohydrazide ***10c.*** White powder, yield 70.5%, m.p.: 189–191 °C FT-IR (KBr (υ_{max}/ cm^{-1}): 3413–3336 (NH pyrimidine, NH hydrazone), 1681 (C═O amide), 3020 (CH aromatic); ^{1}H NMR (DMSO-d_6, 400 MHz) δ = 2.34 (s, 3H, —CH_3—), 5.85 (s, 1H, Ar-H), 7.53,7.55 (d, J = 8.00 Hz, 1H, Ar-H), 7.72 (s, 1H, Ar-H), 8.03, 8.05 (d, J = 8.00 Hz, 1H, Ar-H), 9.01 (s, 1*H*, —N═C*H*—), 12.51 (s, 1H, cyclic —NH—, D_2O exchangeable), 13.36 (s, 1H, —NH—, D_2O exchangeable); EIMS *m/z* (%): 363.65 [M^+−H] (18.84), 366.93 [M+2] (5.60), 276.34 (100); Elemental analysis calculated for $C_{14}H_{10}Cl_2N_6O_2$ (365.17) C, 46.05; H, 2.76; N, 23.01; Found C, 46.02; H,2.75; N,23.00.

4.1.4. 2-(5-Methyl-7-oxo-4,7-dihydro-[1,2,4]triazolo[1,5-a]pyrimidine-2-carbonyl)-N-phenylhydrazinecarbothioamide ***11***

Phenyl isothiocynate (0.0009 mol) was added to a solution of compound **9** (0.0009 mol) in absolute ethanol (20 mL) and heated under reflux for 3 h. The reaction mixture was concentrated under reduced pressure; the product was collected and re-crystallized from ethanol to give the corresponding compound **11**.

White powder, yield 90%, m.p.: 227–229 °C FT-IR (KBr (υ_{max}/ cm^{-1}): 3280–3265 (NH pyrimidine, NH amidic), 1667 (C═O amide), 3055 (CH aromatic), 1522 (C═S); ^{1}H NMR (DMSO-d_6, 400 MHz) ^{1}H NMR (DMSO-d_6, 400 MHz) δ = 2.30 (s, 3H, —CH_3—), 3.46 (s, 1H, —NH—, D_2O exchangeable), 5.77 (s, 1H, Ar-H), 7.10–7.33 (m,5H, Ar-H), 7.53 (s, 1H, —NH—, D_2O exchangeable), 9.46 (s, 2H, —NH—, D_2O

exchangeable); ^{13}C NMR (DMSO-d_6):(100 MHz) δ = 20.94, 98.06, 98.07, 128.49, 154.99, 155.28, 155.89, 156.92, 157.05, 158.98; DEPT C^{135} ($CDCl_3$, 100 MHz, δ ppm); 20.93 (pyrimidine C*H*$_3$-5), 98.10 (pyrimidine C*H*-6), 117.24 (phenyl C*H*-2 + C*H*-6), 121.49 (phenyl C*H*-3 + C*H*-5), 128.46 (phenyl C*H*-4); EIMS *m/z* (%): 343.70 [M$^+$] (3.20), 131.20 (100); Elemental analysis calculated for $C_{14}H_{13}N_7O_2S$ (343.36) C, 48.97; H, 3.82; N, 28.55; Found C,48.97; H,3.81; N,28.54.

4.1.5. General procedure for the synthesis of compounds ***12a,b***

A mixture of compound **4** (0.007 mol), appropriate aliphatic amine (0.0021 mol) and triethylamine (0.005 mol) was heated under reflux for 6 h. Then, triethylamine and excess aliphatic amine were distilled off in a vacuum; 2–3 mL of water was added to the residue; the precipitate was filtered off and re-crystallized from water to offer compounds **12a,b**.

4.1.5.1. 5- Amino-N-(4-methylpiperazin-1-yl)-1H-1,2,4-triazole-3-carboxamide ***12a.*** yellow powder, yield: 30.6%, m.p.: 279–281 °C; FT-IR (KBr (υ_{max}/ cm^{-1}): 3459 (forked NH_2), 3433 (NH), 1651 (C═O amide); ^{1}H NMR (DMSO-d_6, 400 MHz) δ = 1.27 (s,3H,N-C*H*$_3$), 3.72–3.75 (t, *J* = 12.00 Hz, 4H, piperazine), 4.23–4.25 (t, *J* = 8.00 Hz, 4H, piperazine), 6.13 (s,2H,NH_2),12.66 (s, 1*H*, cyclic —NH—, D_2O exchangeable); EIMS *m/z* (%): 225.72 [M$^+$] (83.20), 142.25 (100); Elemental analysis calculated for $C_8H_{15}N_7O$ (225.25) C, 42.66; H, 6.71; N, 43.53; Found C, 42.45; H, 6.58; N, 43.74.

4.1.5.2. (5-Amino-1H-1,2,4-triazol-3-yl)(morpholino)methanone ***12b.*** White powder, yield: 33.7%, m.p.: 269–271 °C; FT-IR (KBr (υ_{max}/ cm^{-1}): 3328 (forked NH_2), 3272 (NH), 1659 (C═O amide), 3055 (CH aromatic); ^{1}H NMR (DMSO-d_6, 400 MHz) δ = 2.59–2.64 (t, *J* = 10.00 Hz, 4H,-morpholine), 3.17–3.22 (t, *J* = 10.00 Hz, 4H,-morpholine), 5.98 (s,2H,NH_2), 13.5 (s, 1*H*, cyclic —NH—, D_2O exchangeable); ^{13}C NMR (DMSO-d_6):(100 MHz) δ = 42.52, 66.93, 138.94, 157.74, 158.69; EIMS *m/z* (%): 197.23 [M$^+$] (36.70), 124.88 (100); Elemental analysis calculated for $C_7H_{11}N_5O_2$ (197.19) C, 42.64; H, 5.62; N, 35.51; Found C, 42.43; H, 5.46; N, 35.36.

4.1.6. General procedure for the synthesis of compounds ***13a-c***

A mixture of compound **4** (0.007 mol), appropriate aromatic amine (0.05 mol) and ammonium chloride (0.005 mol) was heated under reflux for 7 h. Then, the excess amine was distilled off under reduced pressure; the residue was collected and re-crystallized from water to offer compounds **13a-c**.

4.1.6.1. 5- Amino-N-phenyl-1H-1,2,4-triazole-3-carboxamide ***13a.*** Brown powder, yield: 42.5%, m.p.: 254–256 °C; FT-IR (KBr (υ_{max}/ cm^{-1}): 3479 (forked NH_2), 3447 (NH), 1693 (C═O amide); ^{1}H NMR (DMSO-d_6, 400 MHz) δ = 6.20 (s,2H,NH_2), 7.09–7.79 (m, 5H, Ar-H), 9.90 (s, 1*H*, —NH—, D_2O exchangeable), 12.59 (s, 1H, cyclic —NH—, D_2O exchangeable); ^{13}C NMR (DMSO-d_6):(100 MHz) δ = 120.56, 128.80, 129.26, 138.94, 154.87, 157.74, 158.69; DEPT C^{135} ($CDCl_3$, 100 MHz, δ ppm); 120.54 (phenyl C*H*-2 + C*H*-6), 128.08 (phenyl C*H*-4), 124.09 (phenyl C*H*-3 + C*H*-5); EIMS *m/z* (%): 203.00 [M$^+$] (34.85), 173.46 (100); Elemental analysis calculated for $C_9H_9N_5O$ (203.20) C,53.20;H,4.46;N,34.47; Found C,53.42;H,4.66;N,34.68.

4.1.6.2. 5- Amino-N-(4-fluorophenyl)-1H-1,2,4-triazole-3-carboxamide ***13b.*** Reddish brown powder, yield: 74.4%, m.p.: 222–224 °C; FT-IR (KBr (υ_{max}/ cm^{-1}): 3225 (forked NH_2), 3353 (NH), 1692 (C═O amide); ^{1}H NMR (DMSO-d_6, 400 MHz) δ = 6.13 (s,2H,NH_2), 7.16, 7.18 (d, *J* = 8.00 Hz, 2H, Ar-H), 7.81, 7.83 (d, *J* = 8.00 Hz, 2H, Ar-H), 10.03 (s, 1*H*, —NH—, D_2O exchangeable), 12.56 (s, 1H, cyclic —NH—, D_2O exchangeable); ^{13}C NMR (DMSO-d_6):(100 MHz) δ = 115.71, 122.46, 135.42, 154.99, 157.63, 158.76, 159.91; DEPT C^{135} ($CDCl_3$, 100 MHz, δ ppm); 115.71 (phenyl C*H*-3 + C*H*-5), 122.45 (phenyl C*H*-2 + C*H*-6); EIMS *m/z* (%): 221.01 [M$^+$] (52.06), 106.24 (100); Elemental analysis calculated for $C_9H_8FN_5O$ (221.19) C, 48.87; H, 3.65; F, 8.59; N, 31.66; Found C,48.95;H,3.38;N,31.49.

4.1.6.3. 5- Amino-N-(4-nitrophenyl)-1H-1,2,4-triazole-3-carboxamide ***13c.*** yellow powder, yield: 70.4%, m.p.: 261–263 °C; FT-IR (KBr (υ_{max}/ cm^{-1}): 3420 (forked NH_2), 3309 (NH), 1686 (C═O amide); ^{1}H NMR (DMSO-d_6, 400 MHz) δ = 6.11 (s,2H,NH_2), 6.60, 6.62 (d, *J* = 8.00 Hz, 2H, Ar-H), 7.92, 7.94 (d, *J* = 8.00 Hz, 2H, Ar-H), 10.07 (s, 1*H*, —NH—, D_2O exchangeable), 12.54 (s, 1H, cyclic —NH—, D_2O exchangeable); Elemental analysis calculated for $C_9H_8N_6O_3$ (248.20) C, 43.55; H, 3.25; N, 33.86; Found C, 43.22; H, 3.43; N, 33.57.

4.1.7. General procedure for the synthesis of compounds ***14a,b***

A solution of compounds **13a,b** (0.001 mol) and ethyl acetoacetate (0.002 mol) in glacial aceic acid (10 mL) was heated under reflux for 7 h. Then, the excess solvent was distilled off under reduced pressure and the residue was re-crystallized from ethanol to offer compounds **14a, b**.

4.1.7.1. 5-Methyl-7-oxo-N-phenyl-4,7-dihydro-[1,2,4]triazolo[1,5-a]pyrimidine-2-carboxamide ***14a.*** White powder, yield 83.5%, m.p.: 178–180 °C FT-IR (KBr (υ_{max}/ cm^{-1}): 3356–3210 (NH pyrimidine, NH amidic), 1681 (C═O amide), 3035 (CH aromatic); ^{1}H NMR (DMSO-d_6, 400 MHz) δ = 2.38 (s, 3H, —CH_3—), 5.96 (s, 1H, Ar-H), 7.11–7.83 (m, 5H, Ar-H), 10.19 (s, 1*H*, —NH, D_2O exchangeable), 11.73 (s, 1H, cyclic —NH—, D_2O exchangeable); ^{13}C NMR (DMSO-d_6):(100 MHz) δ = 19.26, 99.27, 121.11, 129.10, 129.4, 138.63, 138.82, 151.55, 152.97, 156.70, 157.8; DEPT C^{135} ($CDCl_3$, 100 MHz, δ ppm); 19.27 (pyrimidine C*H*$_3$-5), 99.28 (pyrimidine C*H*-6), 120.78 (phenyl C*H*-2 + C*H*-6), 124.74 (phenyl C*H*-4), 129.15 (phenyl C*H*-3 + C*H*-5); EIMS *m/z* (%): 269.36 [M$^+$] (29.78), 116.69 (100); Elemental analysis calculated for $C_{13}H_{11}N_5O_2$ (269.26) C, 57.99; H, 4.12; N, 26.01; Found C,57.98; H,4.11; N,26.01.

4.1.7.2. N-(4-Fluorophenyl)-5-methyl-7-oxo-4,7-dihydro-[1,2,4]triazolo [1,5-a]pyrimidine-2-carboxamide ***14b.*** White powder, yield 86.8%, m.p.: 169–171 °C FT-IR (KBr (υ_{max}/ cm^{-1}): 3394–3354 (NH pyrimidine, NH amidic), 1682 (C═O amide), 3025 (CH aromatic); ^{1}H NMR (DMSO-d_6, 400 MHz) δ = 2.38 (s, 3H, —CH_3—), 5.96 (s, 1H, Ar-H), 7.19,7.21 (d, *J* = 8.00 Hz, 2H, Ar-H), 7.86, 7.88 (d, *J* = 8.00 Hz, 2H, Ar-H), 10.32 (s, 1*H*, —NH—, D_2O exchangeable), 11.72 (s, 1H, cyclic —NH—, D_2O exchangeable); ^{13}C NMR (DMSO-d_6):(100 MHz) δ = 19.26, 99.27, 120.78, 129.10, 129.14, 138.63, 138.82, 151.55, 152.97, 156.70, 157.87; DEPT C^{135} ($CDCl_3$, 100 MHz, δ ppm); 19.28 (pyrimidine C*H*$_3$-5), 99.28 (pyrimidine C*H*-6), 115.55 (phenyl C*H*-3 + C*H*-5), 122.64 (phenyl C*H*-2 + C*H*-6); EIMS *m/z* (%): 287.39 [M$^+$] (30.57), 96.68 (100); Elemental analysis calculated for $C_{13}H_{10}FN_5O_2$ (287.25) C, 54.36; H, 3.51; N, 24.38; Found C,54.35; H,3.50; N,24.37.

4.2. Biological evaluation

The antimicrobial screening and cytotoxicity studies were performed at CO-ADD (The Community for Antimicrobial Drug Discovery), funded by the Wellcome Trust (UK) and The University of Queensland, Australia **(Supplementary M1).**

4.2.1. Antibacterial assay

All bacteria were cultured in cation-adjusted Mueller Hinton broth (CAMHB) at 37 °c overnight. A sample of each culture was then diluted 40-fold in fresh broth and incubated at 37 °c for 1.5–3 h. The resultant mid-log phase cultures were diluted (CFU/mL measured by OD_{600}), then added to each well of the compound containing plates, giving a cell density of 5x10^5 CFU/mL and a total volume of 50 μL. All the plates were covered and incubated at 37 °C for 18 h without shaking [27].

4.2.2. Antifungal assay

Fungi strains were cultured for 3 days on Yeast Extract-Peptone

Dextrose (YPD) agar at 30 °C. A yeast suspension of 1×10^6 to 5×10^6 CFU/mL (as determined by OD530) was prepared from five colonies. The suspension was subsequently diluted and added to each well of the compound-containing plates giving a final cell density of fungi suspension of 2.5 x10^3 CFU/mL and a total volume of 50 μL. All plates were covered and incubated at 35 °C for 24 h without shaking [9,10].

4.2.3. Cytotoxicity against human embryonic kidney cell line

HEK293 cells were counted manually in a Neubauer hemocytometer and then plated in the 384-well plates containing the compounds to give a density of 5000 cells/well in a final volume of 50 μL. DMEM supplemented with 10% FBS was used as growth media and the cells were incubated together with compounds for 20 h at 37 °C in 5% CO_2 [9,10].

4.2.4. Hemolysis of human red blood cells

Human whole blood was washed three times with 3 volumes of 0.9% NaCl and then suspended in the same concentration of 0.5×10^8 cells/mL, as determined by manual cell count in Neubauer hemocytometer. The washed cells were then added to the 384-well compound-containing plates for a final volume of 50 μL. After a 10 min shake on a plate shaker the plates were then incubated for 1 h at 37 °C. After incubation, the plates were centrifuged at 1000 g for 10 min to pellet cells and debris, 25 μL of the supermatant was then transferred to polystyrene 384-well assay plate [9,10].

4.2.5. Inhibition of lanosterol 14α-demethylase (CYP51) activity

Compounds **9, 13a** and **13b** were screened for their inhibitiory activity of lanosterol 14α-demethylase (CYP51) at Confirmatory Diagnostic Unit, VACSERA, Cairo, Egypt **(Supplementary M2)**. Since resorufin and 7-ethoxyresorufin are light sensitive, the experiment was carried out under yellow light in order to protect the integrity of the stock solutions. Incubations were set up in a black 96-well plate and consisted of substrate (7ER) and CYP1A2 Bactosomes in phosphate buffer containing magnesium chloride. Reactions were initiated by adding 40 μL of 5x NADPH generating system (this can be omitted from wells containing blanks and standards). Metabolite (resorufin) formation was measured fluorometrically, using detection wavelengths chosen to minimize interference from NADPH and 7ER. The substrate, 7-ethoxyresorufin and metabolite (resorufin) were available from Cypex [9].

4.3. In-silico studies

4.3.1. Molecular docking

The 3D structures of the compounds **9, 13a** and **13b** were drawn using the MOE software (Chemical Computing Group software, Canada 2020.01) drawing tool bar [34]. The lowest energy conformer of the compounds (global-minima) was docked into the active site of lansterol 14α-demethylase, which was complexed with fluconazole (PDB ID: 1EA1).The Ligx option was used to structure synthesis, correction and 3D protonation with refinement RMSD gradient to 0.1 kcal/mol/Ao. The molecular mechanics force field 'MMFF94x' was used for energy minimization of each compound. The most active compounds, which were docked into the active site of lansterol 14α-demethylase (a cytochrome *P*-450 enzyme), revealed significant inhibition of the enzyme, in a comparable pattern to that of co-crystalized ligand (fluconazole). The binding energy was calculated as the difference between the energy of the complex and individual energies of the enzyme and ligand. The compounds under study were subjected to flexible alignment experiment using 'Molecular Operating Environment' software (MOE of Chemical Computing Group Inc., on a Core i5 2.2 GHz workstation). Docking validation was performed to ensure the validity of the protocol. The re-docked ligand exhibited a value of rmsd 0.8 between the co-crystalized ligand and the docked structure. Poses for compounds **9, 13a** and **13b** were scored by initial and final rescoring methodology (London dG). Then docking was performed by using template placement refinement with rigid receptor and finally the best scoring pose of the docked compound, receptor-ligand interactions of the complexes were examined, Figs. 2 and 3.

4.3.2. Computational analysis: Prediction of physicochemical properties, pharmacokinetics and drug-likeness profile

Computational studies for predicted pharmacokinetics/ pharmacodynamics properties and toxicity of the most active compounds (**9, 13a** and **13b)** have been performed online to investigate their ADMET (absorption, distribution, metabolism, elimination, and toxicity) profiles [35–42]. The present research tools included pre-ADMET (https://preadmet.bmdrc.kr) [35,36] Molinspiration (https://www.molinspiration.com) [37,38], Molsoft (https://molsoft.com) [39] and SwissADME, (http://www.swissadme.ch) [40–42].

Declaration of Competing Interest

The authors declare that they have no known competing financial interests or personal relationships that could have appeared to influence the work reported in this paper.

Acknowledgment

Authors are grateful to CO-ADD (The Community for Antimicrobial Drug Discovery) Australia, funded by the Wellcome Trust (UK) and The University of Queensland (Australia) for performing the antimicrobial screening.

Funding sources

This research did not receive any specific grant from funding agencies in the public, commercial, or not-for-profit sectors.

Appendix A. Supplementary material

Supplementary data to this article can be found online at https://doi.org/10.1016/j.bioorg.2021.104841.

References

[1] R. Patini, G. Mangino, L. Martellacci, G. Quaranta, L. Masucci, P. Gallenzi, The effect of different antibiotic regimens on bacterial resistance: A systematic review, Antibiotics 9 (2020) 22, https://doi.org/10.3390/antibiotics9010022.
[2] T.M. Belete, Novel targets to develop new antibacterial agents and novel alternatives to antibacterial agents, Hum. Microbiome J. 11 (2019) 100052, https://doi.org/10.1016/j.humic.2019.01.001.
[3] H.K. Mahmoud, B.H. Asghar, M.F. Harras, T.A. Farghaly, Nano-sized formazan analogues: Synthesis, structure elucidation, antimicrobial activity and docking study for COVID-19, Bioorg. Chem. 105 (2020) 104354, https://doi.org/10.1016/j.bioorg.2020.104354.
[4] J. Dai, R. Han, Y. Xu, N. Li, J. Wang, W. Dan, Recent progress of antibacterial natural products: Future antibiotics candidates, Bioorg. Chem. 101 (2020) 103922, https://doi.org/10.1016/j.bioorg.2020.103922.
[5] S.M. Mansura, E.K. Ekta, N.K. Shital, S.T. Madhumita, R.P. Karishma, Emerging strategies to combat ESKAPE pathogens in the era of antimicrobial resistance: A review, Front. Microbiol. 10 (2019) 539, https://doi.org/10.3389/fmicb.2019.00539.
[6] C.L. Skaggs, G.J. Ren, E.T.M. Elgierari, L.R. Sturmer, R.Z. Shi, N.E. Manicke, L. M. Kirkpatrick, Simultaneous quantitation of five triazole anti-fungal agents by paper spray-mass spectrometry, Clin. Chem. Lab. Med. 58 (5) (2020) 836, https://doi.org/10.1515/cclm-2019-0895.
[7] G.I. Lepesheva, F. Villalta, M.R. Waterman, Targeting trypanosoma cruzi sterol 14α-demethylase (CYP51), Adv. Parasitol. 75 (2011) 65, https://doi.org/10.1016/B978-0-12-385863-4.00004-6.
[8] D. Dheer, V. Singh, R. Shankar, Medicinal attributes of 1,2,3-triazoles: Current developments, Bioorg. Chem. 71 (2017) 30, https://doi.org/10.1016/j.bioorg.2017.01.010.
[9] M. M. Morcoss, E. M. N. Abdelhafez, R. A. Ibrahem, H. M. Abdel-Rahman, M. Abdel-Aziz, D. A. Abou El-Ella, Design, Synthesis, Mechanistic studies and in silico ADME predictions of benzimidazole derivatives as novel antifungal agents, Bioorg. Chem. 101 (2020), 103956, https://doi.org/10.1016/j.bioorg.2020.103956.
[10] R.H. Abdel-El-Aleam, R.F. George, G.S. Hassan, H.M. Abdel-Rahman, Synthesis of 1, 2, 4-triazolo [1, 5-a] pyrimidine derivatives: Antimicrobial activity, DNA Gyrase

inhibition and molecular docking, Bioorg. Chem. 94 (2020) 103411, https://doi.org/10.1016/j.bioorg.2019.103411.
[11] F. Yang, L.-Z. Yu, P.-C. Diao, X.-E. Jian, M.-F. Zhou, C.-S. Jiang, W.-W. You, W.-F. Ma, P.-L. Zhao, Novel [1, 2, 4] triazolo [1, 5-a] pyrimidine derivatives as potent antitubulin agents: Design, multicomponent synthesis and antiproliferative activities, Bioorg. Chem. 92 (2019) 103260, https://doi.org/10.1016/j.bioorg.2019.103260.
[12] G.N. Tageldin, T.M. Ibrahim, S.M. Fahmy, H.M. Ashour, M.A. Khalil, R.A. Nassra, I. M. Labouta, Synthesis, modeling and biological evaluation of some pyrazolo[3,4-d] pyrimidinones and pyrazolo[4,3-e][1,2,4]triazolo[4,3-a]pyrimidinones as anti-inflammatory agents, Bioorg. Chem. 90 (2019) 102844, https://doi.org/10.1016/j.bioorg.2019.03.018.
[13] J. Zhuang, S. Ma, Recent Development of pyrimidine- containing antimicrobial agents, Chem. Med. Chem. 15 (2020) 1875, https://doi.org/10.1002/cmdc.202000378.
[14] V. Sharma, N. Chitranshi, A.K. Agarwal, Significance and biological importance of pyrimidine in the microbial world, Int. J. Med. Chem. 2014 (2014) 202784, https://doi.org/10.1155/2014/202784.
[15] T. Wang, S. Yang, H. Li, A. Lu, Z. Wang, Y. Yao, Q. Wang, F., Chemistry, discovery, structural optimization and mode of action of essramycin alkaloid and its derivatives as anti-tobacco mosaic virus and anti-phytopathogenic fungus agents, J. Agric. Food Chem. 68 (2020) 471, https://doi.org/10.1021/acs.jafc.9b06006.
[16] M.M. El-Gendy, M. Shaaban, K.A. Shaaban, A.M. El-Bondkly, H. Laatsch, Essramycin: a first triazolopyrimidine antibiotic isolated from nature, J. Antibiot. 61 (2008) 149, https://doi.org/10.1038/ja.2008.124.
[17] E.H.L. Tee, T. Karoli, S. Ramu, J.X. Huang, M.S. Butler, M.A. Cooper, Synthesis of essramycin and comparison of its antibacterial activity, J. Nat. Prod. 73 (11) (2010) 1940, https://doi.org/10.1021/np100648q.
[18] G. Fischer, Recent advances in 1,2,4-triazolo[1,5-a]pyrimidine chemistry, Adv. Heterocycl. Chem. 128 (2019) 1, https://doi.org/10.1016/bs.aihch.2018.10.002.
[19] K.S. Jain, V.M. Khedkar, N. Arya, P.V. Rane, P.K. Chaskar, E.C. Coutinho, Design, synthesis & evaluation of condensed 2H–4-arylaminopyrimidines as novel antifungal agents, Eur. J. Med. Chem. 77 (2014) 166, https://doi.org/10.1016/j.ejmech.2014.02.066.
[20] S. Ahmed, M.F. Zayed, S.M. El-Messery, M.H. Al-Agamy, H.M. Abdel-Rahman, Design, synthesis, antimicrobial evaluation and molecular modeling study of 1,2,4-triazole-based 4- thiazolidinones, Molecules 21 (2016) 568, https://doi.org/10.3390/molecules21050568.
[21] M. Fesatidou, A. Petrou, G. Athina, Heterocycle compounds with antimicrobial activity, Curr. Pharm. Des. 26 (2020) 867, https://doi.org/10.2174/1381612826666200206093815.
[22] T. Panneerselvam, J.R. Mandhadi, Microwave assisted synthesis and antimicrobial evaluation of novel substituted thiosemicarbazide derivatives of pyrimidine, J. Heterocycl. Chem. 57 (2020) 3082, https://doi.org/10.1002/jhet.4013.
[23] R. Jin, C. Zeng, X. Liang, X.-Hong Sun, Y. Liu, Y. Wang, S. Zhou, Design, synthesis, biological activities and DFT calculation of novel 1,2,4-triazole Schiff base derivatives, Bioorg. Chem. 80 (2018), 253, https://doi.org/10.1016/j.bioorg.2018.06.030.
[24] B. Wang, L. Zhang, X. Liu, Y. Ma, Y. Zhang, Z. Li, X. Zhang, Synthesis, biological activities and SAR studies of new 3-substitutedphenyl-4-substitutedbenzylideneamino-1,2,4-triazole Mannich bases and bis-Mannich bases as ketol-acid reductoisomerase inhibitors, Bioorg. Med. Chem. Lett. 27 (2017) 5457, https://doi.org/10.1016/j.bmcl.2017.10.065.
[25] H. Bayrak, A. Demirbas, S.A. Karaoglu, N. Demirbas, Synthesis of some new 1, 2, 4-triazoles, their Mannich and Schiff bases and evaluation of their antimicrobial activities, Eur. J. Med. Chem. 44 (2009) 1057, https://doi.org/10.1016/j.ejmech.2008.06.019.
[26] A.A. Abd-Elhafez, H.M. Mohamed, H.Y. Hassan, G.S. El-Karamany, N.A. El-Koussi, A.F. Youssef, Synthesis and investigation of certain 3(5)-substituted-1,2,4-triazole-5(3)-carboxylic acid deivatives, Bull. Pharm. Sci. Assiut 20 (1997) 47, 10.21608/BFSA.1997.68738.
[27] A. Kamal, S.M.A. Hussaini, M.L. Sucharita, Y. Poornachandra, F. Sultana, C. G. Kumar, Synthesis and antimicrobial potential of nitrofuran–triazole congeners, Org. Biomol. Chem. 13 (2015) 9388, https://doi.org/10.1039/C5OB01353D.
[28] K. Lal, N. Poonia, P. Rani, A. Kumar, A. Kumar, Design, synthesis, antimicrobial evaluation and docking studies of urea-triazole-amide hybrids, J. Mol. Struct. 1215 (2020) 128234, https://doi.org/10.1016/j.molstruc.2020.128234.
[29] F. Gao, L. Ye, F. Kong, G. Huang, J. Xiao, Design, synthesis and antibacterial activity evaluation of moxifloxacin-amide-1,2,3-triazole-isatin hybrids, Bioorg. Chem. 91 (2019) 103162, https://doi.org/10.1016/j.bioorg.2019.103162.
[30] Y.A. Titova, O. Fedorova, G. Rusinov, V. Charushin, Three-component green synthesis of 6-ethoxycarbonyl-5-methyl-7-(thien-2-yl)-4, 7-dihydro [1, 2, 4] triazolo [1, 5-a] pyrimidine, a promising antituberculosis drug, Russ. Chem. Bull. 68 (2019) 2271, https://doi.org/10.1007/s11172-019-2698-6.
[31] H.M. Ashour, O.G. Shaaban, O.H. Rizk, I.M. El-Ashmawy, Synthesis and biological evaluation of thieno [2′, 3′: 4, 5] pyrimido [1, 2-b][1, 2, 4] triazines and thieno [2, 3-d][1, 2, 4] triazolo [1, 5-a] pyrimidines as anti-inflammatory and analgesic agents, Eur. J. Med. Chem. 62 (2013) 341, https://doi.org/10.1016/j.ejmech.2012.12.003.
[32] K.R.A. Abdellatif, A. Belal, M.T. El-Saadi, N.H. Amin, E.G. Said, L.R. Hemeda, Design, synthesis, molecular docking and antiproliferative activity of some novel benzothiazole derivatives targeting EGFR/HER2 and TS, Bioorg. Chem. 101 (2020) 103976, https://doi.org/10.1016/j.bioorg.2020.103976.
[33] E. Masiukiewicz, B. Rzeszotarska, I.W. Gorczyca, E. Kołodziejczyk, Peptide synthesis with 5-Amino-1-methyl-1H-[1,2,4]triazole-3-carboxylic Acid, Synth. Commun. 37 (11) (2007) 1917, https://doi.org/10.1080/00397910701341423.
[34] A.A. Radwan, F.K. Alanazi, M.H. Al-Agamy, 1, 3, 4-Thiadiazole and 1, 2, 4-triazole-3 (4 H)-thione bearing salicylate moiety: synthesis and evaluation as anti-Candida albicans, Brazilian J. Pharm. Sci. 53 (2017) e15239, https://doi.org/10.1590/s2175-97902017000115239.
[35] D.E.V. Pires, T.L. Blundell, D.B. Ascher, pkCSM: Predicting small- molecule pharmacokinetic and toxicity properties using graph- based signatures, J. Med. Chem. 58 (2015) 4066, https://doi.org/10.1021/acs.jmedchem.5b00104.
[36] N.H. Amin, M.T. Elsaadi, S.S. Zaki, H.M. Abdel-Rahman, Design, synthesis and molecular modeling studies of 2-styrylquinazoline derivatives as EGFR inhibitors and apoptosis inducers, Bioorg. Chem. 105 (2020) 104358, https://doi.org/10.1016/j.bioorg.2020.104358.
[37] Molinspiration cheminformatics, www.molinspiration.com/services/properties.html.
[38] A. H. Abdelazeem,A. G. Safi El-Din, M. M. Abdel-Fattah, N. H. Amin, S. M. El-Moghazy, M. T. El-Saadi, Eur. J. Med. Chem. 205 (2020), 112662, https://doi.org/10.1016/j.ejmech.2020.112662.
[39] MolSoft, https://www.molsoft.com/download.html.
[40] A. Daina, O. Michielin, V. Zoete, SwissADME: a free web tool to evaluate pharmacokinetics, drug-likeness and medicinal chemistry friendliness of small molecules, Sci. Rep. 7 (2017) 42717, https://doi.org/10.1038/srep42717.
[41] C.A. Lipinski, F. Lombardo, B.W. Dominy, P.J. Feeney, Experimental and computational approaches to estimate solubility and permeability in drug discovery and development settings, Adv. Drug Deliv. Rev. 64 (2012) 4, https://doi.org/10.1016/j.addr.2012.09.019.
[42] C.-Y. Jia, J.-Y. Li, G.-F. Hao, G.-F. Yang, A drug-likeness toolbox facilitates ADMET study in drug discovery, Drug Discov. Today 25 (2020) 248, https://doi.org/10.1016/j.drudis.2019.10.014.